AEM
Journals.ASM.org

# The Zeamine Antibiotics Affect the Integrity of Bacterial Membranes

**Joleen Masschelein,[a,b] Charlien Clauwers,[a,b] Karen Stalmans,[a] Koen Nuyts,[c] Wim De Borggraeve,[c] Yves Briers,[a] Abram Aertsen,[b] Chris W. Michiels,[b] Rob Lavigne[a]**

Laboratory of Gene Technology, Department of Biosystems,[a] Laboratory of Food Microbiology, Department of Microbial and Molecular Systems,[b] and Molecular Design and Synthesis, Department of Chemistry,[c] KU Leuven, Heverlee, Belgium

**The zeamines (zeamine, zeamine I, and zeamine II) constitute an unusual class of cationic polyamine-polyketide-nonribosomal peptide antibiotics produced by *Serratia plymuthica* RVH1. They exhibit potent bactericidal activity, killing a broad range of Gram-negative and Gram-positive bacteria, including multidrug-resistant pathogens. Examination of their specific mode of action and molecular target revealed that the zeamines affect the integrity of cell membranes. The zeamines provoke rapid release of carboxyfluorescein from unilamellar vesicles with different phospholipid compositions, demonstrating that they can interact directly with the lipid bilayer in the absence of a specific target. DNA, RNA, fatty acid, and protein biosynthetic processes ceased simultaneously at subinhibitory levels of the antibiotics, presumably as a direct consequence of membrane disruption. The zeamine antibiotics also facilitated the uptake of small molecules, such as 1-N-phenylnaphtylamine, indicating their ability to permeabilize the Gram-negative outer membrane (OM). The valine-linked polyketide moiety present in zeamine and zeamine I was found to increase the efficiency of this process. In contrast, translocation of the large hydrophilic fluorescent peptidoglycan binding protein $PBD_{KZ}$-GFP was not facilitated, suggesting that the zeamines cause subtle perturbation of the OM rather than drastic alterations or defined pore formation. At zeamine concentrations above those required for growth inhibition, membrane lysis occurred as indicated by time-lapse microscopy. Together, these findings show that the bactericidal activity of the zeamines derives from generalized membrane permeabilization, which likely is initiated by electrostatic interactions with negatively charged membrane components.**

Bacterial secondary metabolites represent an enormous group of natural products that do not play an essential role in normal growth and development of an organism but confer a selective advantage in certain ecological niches and complex microbial communities (1). Production of these metabolites typically occurs at the onset of stationary growth phase and may be triggered by specific environmental stimuli. Because of their structural diversity and complexity, secondary metabolites exhibit an impressive array of biological activities and may act as metal transporters, toxins, bioregulators, antimicrobial agents, enzyme inhibitors, insecticides, and signaling compounds. The genes for their biosynthetic pathways are typically clustered in the genome together with genes for resistance, export, and postassembly tailoring (2). Secondary metabolites are classified into different groups based on their biosynthetic origin and chemical structure. These include polyketides, terpenes, alkaloids, nonribosomal peptides, and lipids.

The zeamines are a class of bioactive polyamine-polyketide-nonribosomal peptide natural products produced by *Serratia plymuthica* RVH1 (3–5). Zeamine and zeamine I consist of a specific valine-linked polyketide moiety, conjugated via an amide bond to a common 40-carbon penta amino hydroxyalkyl chain (zeamine II) (Fig. 1). The 50-kb zeamine biosynthetic gene cluster has been identified in the genome of *S. plymuthica* RVH1 and consists of 15 coding sequences. Besides tailoring and export-related enzymes, the gene cluster encodes two separate enzymatic assembly lines for the biosynthesis of the polyamino alcohol chain and the peptide-polyketide moiety (4). Recently, the pathway for zeamine biosynthesis, which involves an unprecedented interaction between nonribosomal peptide synthetase, type I modular polyketide synthase, and polyunsaturated fatty acid synthase-like biosynthetic machinery, was fully characterized (6). Zeamine and zeamine II also have been reported as metabolites of the bacterial phytopathogen *Dickeya zeae* EC1 (7), and homology searches indicate that the biosynthetic gene cluster is conserved among several other *Enterobacteriaceae* genera, e.g., *Photorhabdus* and *Xenorhabdus*.

All components of the zeamine complex are cationic at physiological pH and exhibit potent bactericidal activity against a broad spectrum of Gram-positive and Gram-negative bacteria, including multidrug-resistant pathogens (8). The production of these antibiotics in *S. plymuthica* RVH1 is quorum-sensing regulated and provides the strain with a selective advantage in competitive habitats, such as mixed-species biofilms (9, 10). Zeamine and zeamine II also have been shown to play a major role in the virulence of *D. zeae* EC1, which causes rice foot rot and maize stalk rot diseases. *D. zeae* mutants defective in zeamine production were no longer able to inhibit rice seed germination and growth. In addition, a reduced virulence on Chinese cabbage and potatoes was observed (7).

In this study, we set out to investigate the specific mode of

**Received** 26 September 2014 **Accepted** 24 November 2014
**Accepted manuscript posted online** 1 December 2014
**Citation** Masschelein J, Clauwers C, Stalmans K, Nuyts K, De Borggraeve W, Briers Y, Aertsen A, Michiels CW, Lavigne R. 2015. The zeamine antibiotics affect the integrity of bacterial membranes. Appl Environ Microbiol 81:1139–1146. doi:10.1128/AEM.03146-14.
**Editor:** M. W. Griffiths
Address correspondence to Rob Lavigne, rob.lavigne@biw.kuleuven.be.

doi:10.1128/AEM.03146-14

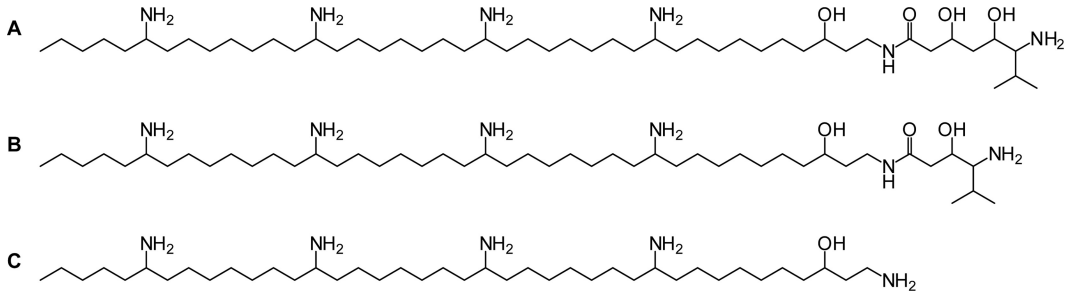


**FIG 1** Structures of zeamine (A), zeamine I (B), and zeamine II (C).

action that underlies the broad-spectrum bactericidal activity of these novel chemical scaffolds. We analyzed the effect of the zeamines on macromolecular synthesis in *Escherichia coli* and *Staphylococcus aureus* and studied their effects at the single-cell level using time-lapse microscopy. We examined the interaction of the zeamines with artificial phospholipid membranes of different compositions by measuring the efflux of encapsulated carboxyfluorescein. The ability of the zeamines to cause outer membrane (OM) permeabilization was characterized by comparing the uptake of small hydrophobic and large hydrophilic probes in *E. coli*. Our results suggest that the zeamines behave in a manner similar to that of cationic antimicrobial peptides, disrupting the integrity of membranes through direct electrostatic and hydrophobic interactions with the phospholipid bilayer.

## MATERIALS AND METHODS

**Chemicals.** Bacto tryptone and yeast extract were purchased from Lab M (Lancashire, United Kingdom). $NH_4SO_2$ and NaCl were purchased from Acros Organics (Geel, Belgium). Radiolabeled precursors and MicroScint were from PerkinElmer (Waltham, MA, USA). Solvents were obtained from Acros Organics. Phospholipids were purchased from Avanti Polar Lipids (Alabaster, AL, USA). All other chemicals were from Sigma-Aldrich (St. Louis, MO, USA).

**Strains and culturing conditions.** *E. coli* MG1655 and *S. aureus* ATCC 27661 were grown and maintained in lysogeny broth (LB) at 37°C. Overnight cultures of *Serratia* sp. strains were made in LB broth and incubated at 30°C. For zeamine production, *S. plymuthica* RVH1 and the *S. plymuthica* RVH1Δ*zmn19* mutant (6) were grown in minimal medium (7) [10.5 g/liter $K_2HPO_4$, 4.5 g/liter $KH_2PO_4$, 2 g/liter $(NH_4)_2SO_4$, 2 g/liter mannitol, 0.2 g/liter $MgSO_4.7H_2O$, 5 mg/liter $FeSO_4$, 10 mg/liter $CaCl_2$, and 2 mg/liter $MnCl_2$; pH 7.0] supplemented with 5 μM synthetic N-(3-oxo-hexanoyl)-$C_6$-homoserine lactone at 16°C for 72 h on a rotary shaker (80 rpm).

**Production and isolation of the zeamine antimicrobial compounds.** Following fermentation of *S. plymuthica* RVH1, cells were removed by centrifugation (4,000 × *g*, 45 min). The supernatant was adjusted to pH 10.0 with 1 M NaOH and extracted with n-butanol twice. The organic solvent was removed by rotary evaporation *in vacuo*. The dry extract was redissolved in methanol (MeOH) containing 5% triethylamine, mixed with three times the amount of silica, and allowed to dry overnight. The silica powder then was added to the top of a silica column and washed sequentially with MeOH-$CH_2Cl_2$ (1:8), MeOH-$CH_2Cl_2$ (1:4), MeOH-$CH_2Cl_2$ (1:2), MeOH-$CH_2Cl_2$ (1:1), and 100% MeOH. The zeamines (a mixture of zeamine, zeamine I, and zeamine II) eluted with MeOH containing 1% formic acid. The fractions of interest were pooled and dried by lyophilization. The dried solids were dissolved either in MeOH or in water for use in cellular assays. The purity of the isolated zeamine compounds was verified by high-performance liquid chromatography (HPLC) and nuclear magnetic resonance (NMR) as described previously (4). For the production and isolation of zeamine II, the *Serratia plymuthica* RVH1Δ*zmn19* mutant (6), deficient in the production of zeamine and zeamine I, was used. Purification was done similarly to that for the zeamine mixture.

**Macromolecular synthesis assay.** The effect of the zeamine antibiotics on DNA, RNA, protein, and lipid synthesis was examined by monitoring the incorporation of radiolabeled precursors [(*methyl*-$^3$H)-thymidine, (5,6-$^3$H)-uridine, L-(4,5-$^3$H)-leucine, (2-$^3$H)-glycerol]. Overnight cultures of *E. coli* MG1655 and *S. aureus* ATCC 27661 were diluted 50-fold in fresh medium and grown to midexponential growth phase (optical density at 600 nm [$OD_{600}$] of 0.3). The $^3$H-labeled precursors then were added to the cells at a final concentration of 1 μCi/ml. The cultures were divided into 96 Deep Well blocks (750 μl/well) with a BREATHseal (Greiner Bio One) on top and incubated at 37°C for 10 min. A mixture of zeamine, zeamine I, and zeamine II (5 mg/ml stock solution in MilliQ water) was subsequently added to the bacterial cultures in final concentrations equivalent to 0.5× and 0.25× the MIC. Negative controls were supplemented with MilliQ water instead of antibiotics. Before and after the addition of the zeamine mixture (time points of 0 min, 10 min, 20 min, 30 min, 45 min, and 60 min), 100-μl samples were taken from the cultures, added to 100 μl ice-cold 10% trichloroacetic acid (TCA), and stored at 4°C for 30 min. The TCA-precipitated samples were transferred to a Unifilter-96 GF/C filter plate (PerkinElmer) by using a Filtermate 196 harvester (Packard). The filter plates were washed four times with 5% TCA, four times with water, and once with 95% ethanol before being dried for 1 min on a 60°C heat block. Finally, 10 μl MicroScint was added to the plates, and scintillation was read with a TopCount NXT microplate scintillation/luminescence counter (PerkinElmer). Experiments were performed in triplicate.

**Preparation of SUVs for CF efflux assays.** Vesicles with the following phospholipid compositions were prepared: (i) 1,2-dioleoyl-*sn*-glycero-3-phosphoethanolamine (DOPE)-1,2-dioleoyl-*sn*-glycero-3-phospho-(1′-*rac*-glycerol) (DOPG) (1-1), (ii) DOPE-DOPG (8-2), and (iii) 1,2-dioleoyl-*sn*-glycero-3-phosphocholine (DOPC)-cholesterol (7-3). Stock solutions (100 mM) of the phospholipids and the cholesterol were made in distilled dichloromethane (DCM) and mixed at the appropriate molar ratios. Solvents were evaporated under nitrogen flow and put in a vacuum desiccator for 3 h to remove trace solvents. The resulting film was rehydrated with a 30 mM carboxyfluorescein (CF) solution in 5 mM HEPES-NaOH buffer, pH 7.4. This solution was vigorously stirred for 15 h in the dark at room temperature and subsequently sonicated at 0°C for 45 min to obtain small unilamellar vehicles (SUVs). Nonencapsulated CF was removed from the liposomes by gel filtration (Sephadex G50 column). Phospholipid concentrations were determined by the inorganic phosphate assay as described by Ames (11). The liposomes were stored at 4°C and used within 48 h.

**CF release assay.** CF release from the SUVs upon exposure to a mixture of zeamine, zeamine I, and zeamine II was evaluated. From a stock solution of 5 mg/ml in MeOH, a 2-fold serial dilution of the zeamine mixture was made in 5 mM HEPES-NaOH buffer, pH 7.4, at 10-fold higher concentrations than the desired final concentration. Liposomal stock preparations were diluted in the same buffer to a final concentration

of 25 μM. Twenty μl of zeamine solution then was added to 180 μl of liposomes in a microwell plate, and the increase in fluorescence intensity was recorded every minute for 20 min in a Fluoroskan Ascent microplate fluorometer (excitation wavelength [$\lambda_{ex}$], 485 nm; emission wavelength [$\lambda_{em}$], 520 nm). As a negative control, buffer was used instead of antibiotics. After 20 min, 20 μl of a 10% Triton X-100 solution was added to the liposomes to solubilize the vesicles and release all trapped CF. The percentage of zeamine-induced CF leakage at time $t$ was calculated as $\%CF = [F(t) - F(0)]/[F(T) - F(0)] \times 100$, where F(0) is fluorescence intensity before addition of zeamines, F($t$) is the fluorescence intensity at time $t$ in the presence of zeamines, and F($T$) is the fluorescence intensity after addition of Triton X-100 (12, 13). Two independent assays were performed, during which each sample was tested in triplicate.

**Cytostatic activity assay.** Murine leukemia L1210, human T-lymphocyte CEM, and human cervix carcinoma (HeLa) cells were suspended at $3 \times 10^5$ to $5 \times 10^5$ cells/ml of culture medium, and 100 μl of a cell suspension was added to 100 μl of an appropriate dilution of the zeamines in wells of 96-well microtiter plates. After incubation at 37°C for two (L1210) or three (CEM and HeLa) days, the cell number was determined using a Coulter counter. The $IC_{50}$ was defined as the compound concentration required to inhibit cell proliferation by 50%.

**Membrane integrity study with fluorescent dyes.** Zeamine-induced membrane damage was assessed with the LIVE/DEAD BacLight bacterial viability kit (Molecular Probes). An overnight culture of *E. coli* MG1655 and *S. aureus* ATCC 27661 was diluted 1:100 in fresh medium and grown to exponential growth phase ($OD_{600}$ of 0.6). Cells were harvested by centrifugation (4,000 × *g*, 20 min), washed with 0.9% NaCl, and resuspended in the same buffer in 1:10 of their original volume. Cells subsequently were diluted 1:20 in 0.9% NaCl containing different final concentrations equivalent to 2× and 4× the MIC of the zeamine mixture (5 mg/ml stock solution in MeOH). MeOH in equivalent concentrations was used as a negative control. Bacteria and test compounds were incubated at room temperature with continuous shaking for 15, 30, or 60 min before being centrifuged at 4,000 × *g* for 20 min. Pellets were washed with 0.9% NaCl and resuspended in half of the previous volume. The resulting bacterial suspension was mixed with the BacLight reagent (3 μl/ml bacterial suspension) and incubated in the dark at room temperature for 15 min. Cells were observed with a fluorescence microscope (Leica DM LB microscope; McBain Instruments) at excitation/emission maxima of 480/500 nm (Syto 9) and 490/635 nm (propidium iodide).

**NPN uptake assay.** Outer membrane permeabilization was evaluated using the 1-N-phenylnaphtylamine (NPN) uptake assay as described previously (14). *E. coli* MG1655 was grown to exponential growth phase ($OD_{600}$ of 0.6) in LB medium at 37°C, washed with 5 mM HEPES-NaOH (pH 7.2), and resuspended in the same buffer at two-thirds of the original volume. Test substances included zeamine II (50 mg/ml stock solution in MeOH) and a mixture of zeamine, zeamine I, and zeamine II (5 mg/ml stock solution in MeOH). To assess a range of concentrations around the MIC of the zeamine mixture (8 μg/ml), serial dilutions of the test compounds were made in 5 mM HEPES-NaOH buffer (pH 7.2). Polymyxin B and kanamycin served as positive and negative controls, respectively, and were dissolved in the same buffer. A 40 mM stock solution of NPN (Sigma-Aldrich) was prepared in acetone and diluted to a concentration of 40 μM in 5 mM HEPES-NaOH buffer (pH 7.2). A 100-μl volume of bacterial suspension was mixed in a microwell plate with 50 μl of the test substance (at a 3-fold higher concentration than the intended final concentration) and incubated at 37°C. After 15 min, 50 μl of NPN (40 μM in 5 mM HEPES-NaOH buffer [pH 7.2]) was added, and fluorescence was read within 3 min. Fluorescence was measured in a Fluoroskan Ascent microplate fluorometer ($\lambda_{ex}$, 355 nm; $\lambda_{em}$, 405 nm; Thermo Labsystems). Optical densities were recorded immediately thereafter with a Multiskan RC (Thermo Labsystems) at 600 nm. Control samples included (i) bacterial suspension (100 μl), buffer (50 μl), and NPN (50 μl); (ii) bacterial suspension (100 μl), test substance (50 μl), and buffer (50 μl); (iii) bacterial suspension (100 μl) and buffer (100 μl); (iv) buffer (150 μl) and NPN (50 μl); and (v) buffer (200 μl). Methanol was included in the buffer in equivalent concentrations when used as a control for the zeamine test compounds. Each sample was tested in triplicate, and independent assays were performed twice. The results were expressed as relative NPN uptake factors (the NPN uptake factor calculated for the test substance, subtracted from the NPN uptake factor calculated for cells without the test substance). To calculate the NPN uptake factor for the test substance, the fluorescence values of the bacterial suspension with the test substance and NPN were divided by the corresponding optical densities and background corrected by subtracting the fluorescence values of control samples without NPN (ii), which were equally divided by their corresponding OD values. The resulting values were then divided by the fluorescence values of the buffer to give the uptake factor. The NPN uptake factor for the cells without test substance was calculated accordingly using the values from control samples containing buffer instead of test substance (i and iii).

**$PBD_{KZ}$-GFP uptake assay.** To examine outer membrane permeability, a fusion protein consisting of the high-affinity N-terminal peptidoglycan binding domain of endolysin KZ144 ($PBD_{KZ}$) from *Pseudomonas aeruginosa* bacteriophage φKZ and green fluorescent protein ($PBD_{KZ}$-GFP) was used (15–17). Bacterial suspensions of *E. coli* MG1655 were prepared as described for the NPN uptake assay. A mixture of zeamine, zeamine I, and zeamine II (10 mg/ml stock solution in MeOH) was used for the assay. To test a range of concentrations around the MIC of the zeamine mixture (8 μg/ml), a dilution series of the antibiotics was made in 5 mM HEPES-NaOH buffer (pH 7.2) in concentrations that were 4-fold higher than the desired final concentration. One hundred microliters of the bacterial suspension was mixed in a microwell plate with 50 μl of the zeamine mixture and 50 μl $PBD_{KZ}$-GFP (final concentration, 0.2 μg/μl). Samples were incubated at room temperature for 15 min. Cells subsequently were collected by centrifugation (13,000 × *g*, 10 min), washed twice in 5 mM HEPES-NaOH, pH 7.2, and resuspended in the same buffer. The fluorescence of $PBD_{KZ}$-GFP was measured in a Fluoroskan Ascent microplate fluorometer ($\lambda_{ex}$, 485 nm; $\lambda_{em}$, 520 nm; Thermo Labsystems). Optical densities were recorded immediately thereafter with a Multiskan RC (Thermo Labsystems) at 600 nm. Control samples included bacterial suspension (100 μl), buffer (50 μl), and $PBD_{KZ}$-GFP (50 μl) (i); bacterial suspension (100 μl), zeamines (50 μl), and buffer (50 μl) (ii); bacterial suspension (100 μl) and buffer (100 μl) (iii); buffer (100 μl), zeamines (50 μl), and $PBD_{KZ}$-GFP (50 μl) (iv); and buffer (200 μl) (v). Methanol was included in the buffer in equivalent concentrations when used as a control for the zeamine mixture. Each sample was tested 3-fold, and independent assays were performed twice. Cells treated with a chloroform-saturated 0.05 M Tris-HCl, pH 7.7, buffer were used as a positive control (18). The results were expressed as relative uptake factors, which were calculated as described for the NPN uptake assay.

**Time-lapse microscopy.** Overnight cultures of *E. coli* MG1655 grown in LB or M medium (19) were diluted 1:100 in fresh medium and spotted on an LB/M medium agar pad containing different final concentrations of the zeamine mixture. Subsequently, the growth of single cells was recorded in real time at 37°C for 4 h with a temperature-controlled (Okolab Ottaviano) Ti-Eclipse inverted microscope (Nikon) equipped with a TI-CT-E motorized condensor and a CoolSnap HQ2 FireWire charge-coupled device (CCD) camera. Images were acquired using NIS Elements AR 3.2 software (Nikon) as described previously (20) and further handled with Fiji open source software (downloaded from http://fiji.sc/Fiji).

## RESULTS

**Rapid and simultaneous inhibition of macromolecular synthesis in *E. coli* and *S. aureus* upon exposure to subinhibitory concentrations of zeamines.** To determine which macromolecular processes are affected by the zeamines, the effect of the antibiotics on the incorporation of [$^3$H]thymidine, [$^3$H]uridine, [$^3$H]leucine, and [$^3$H]glycerol was examined in *E. coli* MG1655. A copurified mixture of zeamine, zeamine I, and zeamine II was added to mid-exponential-phase cultures at a concentration of 4 μg/ml (MIC, 8

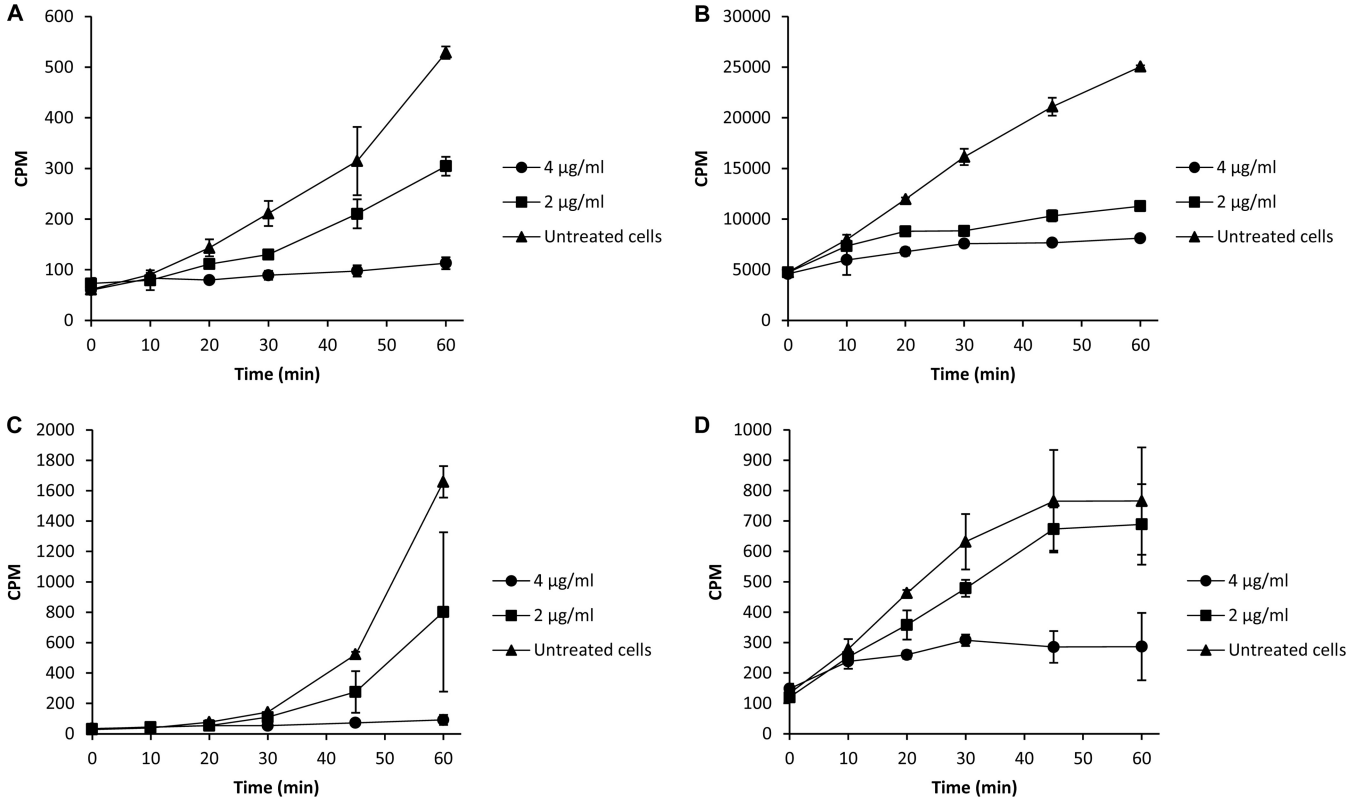


**FIG 2** Impact of the zeamines on the biosynthesis of proteins (A), RNA (B), fatty acids (C), and DNA (D) in *E. coli* MG1655. CPM, counts per minute. Cells were incubated with the antibiotics at concentrations of 2 and 4 μg/ml (MIC, 8 μg/ml) from time zero. Data are represented as means ± standard deviations from triplicate experiments.

μg/ml) (6). Within 20 min, this resulted in the complete and simultaneous inhibition of DNA, RNA, protein, and fatty acid biosynthesis (Fig. 2). In the presence of 2 μg/ml of the zeamine mixture, intermediate inhibition was observed. Comparable effects and kinetics were observed in assays with *S. aureus* (data not shown). The rate and lack of specificity in the inhibition of the macromolecular processes at low dose indicate that DNA, RNA, protein, and fatty acid biosynthesis are not a primary target of the zeamines and suggest that the inhibition is an indirect effect of a more general action of these antimicrobial metabolites. The long, hydrophobic backbone of the zeamines, along with their broad spectrum of activity, led us to investigate their impact on the physical integrity of membranes.

**The zeamines cause nonspecific membrane damage in direct interaction with phospholipid bilayers.** To study the interaction of the zeamine antibiotics with phospholipid bilayers, the release of carboxyfluorescein (CF) from small unilamellar vesicles (SUVs) was monitored (12, 13). As long as CF is entrapped within the SUVs, its fluorescence emission is autoquenched due to a high local concentration. However, when the integrity of the membrane is disrupted, or when the permeability is increased as a result of membrane phase rearrangement, CF dilutes into the environment, resulting in prominent fluorescence. SUVs with different phospholipid compositions (phosphatidylethanolamine/phosphatidylglycerol [PE/PG] ratio of 1:1, PE/PG ratio of 8:2, and phosphatidylcholine/cholesterol [PC/Ch] ratio of 7:3) were prepared to mimic the cytoplasmic membrane of Gram-positive bacteria, Gram-negative bacteria, and human erythrocytes, respectively (21). The addition of increasing amounts of the zeamine mixture, ranging from 1 μg/ml to 32 μg/ml, caused rapid and immediate concentration-dependent CF leakage from both types of PE/PG SUVs tested, followed by a period of slower CF release (Fig. 3). The zeamines were slightly more effective on the PE/PG 8:2 SUVs than on the PE/PG 1:1 vesicles. In contrast, liposomes made of PC/Ch were less affected by the zeamine mixture (<50% release). These results demonstrate the ability of the zeamines to directly interact with bacterial model membranes in the absence of a specific receptor and to permeabilize the phospholipid bilayer. Despite the lower selectivity for eukaryotic model membranes, significant cytostatic activity was observed against murine leukemia cells (L1210), human T-lymphocyte cells (CEM), and human cervix carcinoma cells (HeLa), with $IC_{50}$s of 3.8 ± 0.1, 4.1 ± 0.7, and 1.7 ± 0.1 μM, respectively.

Nonspecific membrane damage following zeamine exposure was confirmed in cultures of *S. aureus* ATCC 27661 and *E. coli* MG1655 using the Live/Dead BacLight bacterial viability kit. Fluorescence microcopy revealed that, in contrast to untreated cells, both cultures uniformly exhibited red fluorescence following treatment with 16 and 32 μg/ml of the zeamine mixture, revealing damage to the cytoplasmic membrane (data not shown).

**Zeamine exposure results in subtle disruption of the outer membrane rather than drastic perturbations or defined pore formation.** Given the antimicrobial activity of the zeamines against Gram-negative bacteria, we subsequently examined the effect of the antibiotics on the permeability of the outer membrane. This was evaluated by monitoring the uptake of the fluo-

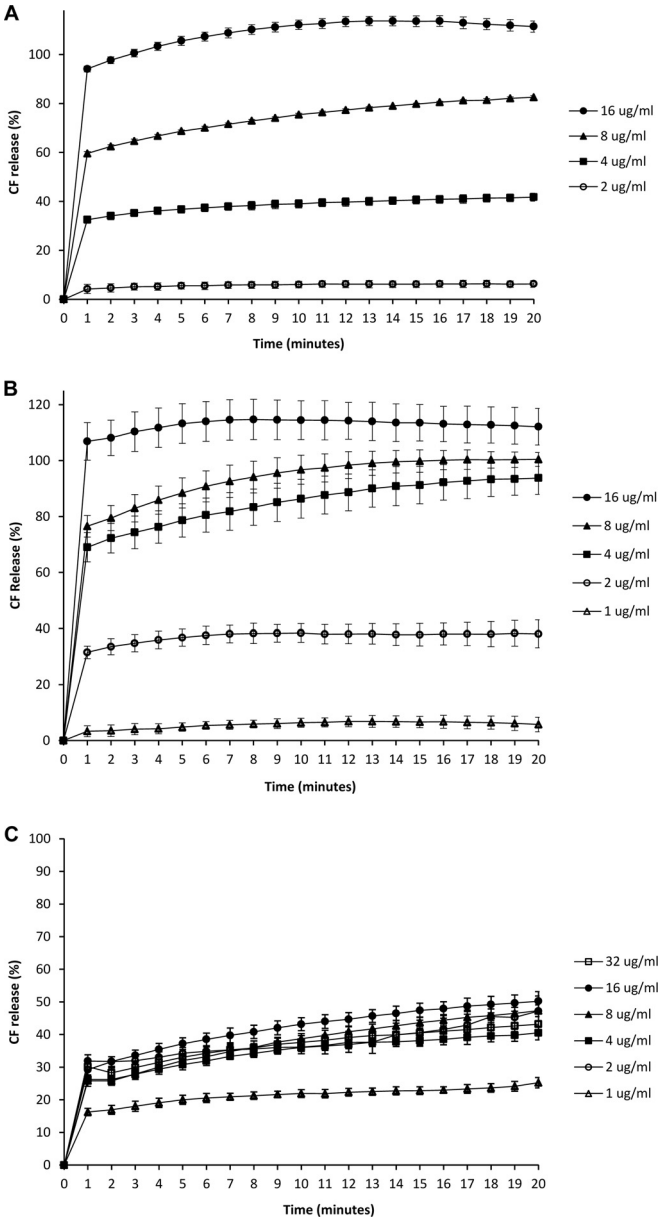


**FIG 3** Zeamine-induced CF leakage from PE/PG 1:1 (A), PE/PG 8:2 (B), and PC/Ch 7:3 (C) SUVs. Antibiotics were added at time zero in different final concentrations, ranging from 1 μg/ml to 32 μg/ml. The SUV concentration was 25 μM.

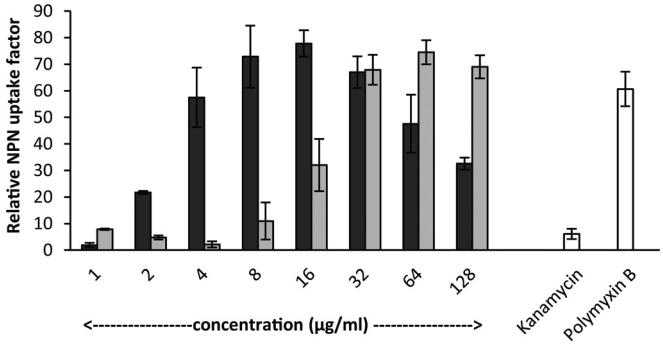


**FIG 4** Effect of different concentrations of a mixture of zeamine, zeamine I, and zeamine II (dark gray bars) and zeamine II alone (light gray bars) on NPN uptake by *E. coli* MG1655. Cells treated with kanamycin (32 μg/ml) and polymyxin B (1 mg/ml) (white bars) served as negative and positive controls, respectively. The results are expressed as relative NPN uptake factors.

rescent probe NPN (14, 22). NPN is a small lipophilic dye which fluoresces strongly in hydrophobic environments and only weakly in aqueous environments. The outer leaflet of the outer membrane is composed mainly of lipopolysaccharide (LPS) molecules, which act as a permeability barrier to external lipophilic substances, like NPN (23). However, when membrane integrity is disrupted, e.g., through the action of a membrane-permeabilizing compound, NPN partitions into the hydrophobic lipid interior of the outer and inner membrane, which results in a strong increase in fluorescence. Exponentially growing *E. coli* MG1655 was incubated with a mixture of zeamine, zeamine I, and zeamine II in different final concentrations, ranging from 1 μg/ml to 128 μg/ml. After 15 min, NPN was added and the samples were read for fluorescence. Polymyxin B, a known membrane-permeabilizing agent, and kanamycin added at their respective MIC values served as a positive and negative control, respectively. The effect of zeamine exposure on NPN uptake by *E. coli* is shown in Fig. 4 as relative NPN uptake factors. The antibiotics clearly affect the integrity of the outer membrane and facilitate NPN uptake to an extent similar to that of polymyxin B. Zeamine-induced membrane permeabilization is dose dependent, requiring a minimum concentration of 2 μg/ml. Maximum NPN uptake was obtained at the MIC (8 μg/ml) (6), and uptake values slowly decreased again at concentrations well above the MIC. Membrane permeabilization also was observed when *E. coli* was incubated with zeamine II alone, albeit at higher concentrations of the antibiotic (Fig. 4). Concentrations above 16 μg/ml were required to induce NPN uptake, and the highest uptake value was obtained after treatment with 64 μg/ml zeamine II. This is in agreement with the lower antimicrobial activity of zeamine II against *E. coli* (MIC, 64 μg/ml) (6) and suggests that the valine-linked polyketide moiety that is missing in zeamine II plays an important role in OM destabilization.

The ability of the zeamines to facilitate the uptake of larger probes was evaluated by using the hydrophilic fluorescent fusion protein $PBD_{KZ}$-GFP, consisting of the N-terminal peptidoglycan-binding domain of endolysin KZ144 ($PBD_{KZ}$) from *Pseudomonas aeruginosa* phage φKZ fused to GFP (15). Normally, $PBD_{KZ}$-GFP cannot access its peptidoglycan substrate unless the outer membrane is drastically damaged. In this case, the fusion protein binds A1γ chemotype peptidoglycan with high affinity. As a consequence, the measured fluorescence intensity directly correlates with the extent of membrane permeabilization. $PBD_{KZ}$-GFP has been used successfully as a tool to evaluate outer membrane permeabilizing agents (16) and to visualize and quantify pressure-induced permeability changes in *P. aeruginosa* PAO1 (17). In this experiment, exponentially growing *E. coli* MG1655 was incubated with $PBD_{KZ}$-GFP and different concentrations of the zeamine mixture. After 15 min, any unbound probes were washed away and fluorescence was recorded. The results, represented as relative uptake factors, are shown in Fig. 5. Unlike the NPN assay, no $PBD_{KZ}$-GFP uptake was observed at concentrations of up to 16 μg/ml. A minimum dose of 32 μg/ml was required to measure

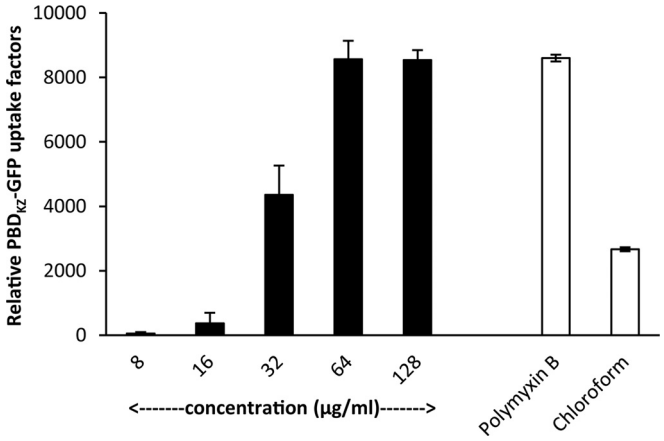


**FIG 5** Zeamine-induced PBD$_{KZ}$-GFP uptake by *E. coli* MG1655 (dark gray bars). Cells treated with polymyxin B (1 mg/ml) and a chloroform-saturated Tris-HCl buffer (white bars) were used as a positive control. Results are represented as relative PBD$_{KZ}$-GFP uptake factors.

fluorescence, and maximal fluorescence was recorded after treatment with 64 μg/ml (8× MIC). However, visualization by fluorescence microcopy revealed that the cells were not homogenously labeled with the probe, contrary to the control chloroform-treated cells (Fig. 6A). Instead, fluorescence originated from aggregates of probe trapped in cellular debris and probe bound to the peptidoglycan of lysed cells (Fig. 6B and C). This phenomenon also was observed with cells treated with 1 mg/ml polymyxin B (data not shown) and explains the elevated uptake PBD$_{KZ}$-GFP values compared to those for chloroform-treated cells. Thus, exposure to high concentrations of zeamines results in membrane solubilization and lysis. These results are consistent with the decline in NPN uptake values observed at the same doses, as discussed in the previous section.

**Time-lapse microscopy reveals morphological changes.** To study the effect of the zeamines at the single-cell level, cell growth and morphological changes of *E. coli* MG1655 were monitored in the presence of antibiotics using time-lapse microscopy. Exposure to zeamines at concentrations of 8 μg/ml completely blocked cell growth, whereas a concentration of 16 μg/ml led to membrane lysis during both cell division and cell growth. Although cells became slightly more spherical, an intact sacculus remained. This indicates that peptidoglycan integrity is not affected and suggests that the lysis is a direct consequence of membrane permeabilization (Fig. 7A). Interestingly, when a similar experiment was performed in M medium, a medium with higher osmolarity (19), a reversible plasmolysis-like phenomenon took place instead of lysis. The cytoplasm shrunk, putatively linked to intracellular content loss, and the cytoplasmic membrane detached from the cell wall. Although this shrinking process appeared to be transient, the cells did not resume growth (Fig. 7B).

## DISCUSSION

This work focused on determining the specific mode of action of the zeamines and identifying their molecular target. Our data reveal that the zeamines cause nonspecific membrane damage in target Gram-positive and Gram-negative bacteria. DNA, RNA, protein, and fatty acid biosynthesis ceased rapidly and simultaneously in the presence of 0.5× MIC of zeamines. This is likely the result of leakage of cellular components or membrane depolarization, causing the depletion of precursors and energy required for these biosynthetic processes. In addition, zeamine treatment may affect the conformation of certain membrane-bound proteins by inducing membrane phase rearrangements. This may in turn trigger signal transduction pathways involved in the regulation of macromolecular processes. The ability of the zeamines to induce carboxyfluorescein leakage from small unilamellar vesicles indicates that they can permeabilize membranes through direct interaction with the phospholipid bilayer and that no receptor-mediated recognition is required. Their higher selectivity for bacterial over eukaryotic model membranes seems to be related to the phospholipid composition and net surface charge of the vesicles. Bacterial phospholipids such as phosphatidylglycerol are negatively charged, facilitating interaction with cationic substances like the zeamines. On the other hand, eukaryotic membranes consist predominantly of zwitterionic phosphatidylcholine and contain cholesterol, which makes the membrane more rigid (24). Despite their lower affinity for artificial eukaryotic membranes, the zeamines were found to exhibit potent antiproliferative activity against murine and human cancer cell lines, with IC$_{50}$s in the 1.7 to 4.1 μM range. The zeamines also were shown to disrupt the Gram-negative OM, facilitating the uptake of the small hydrophobic

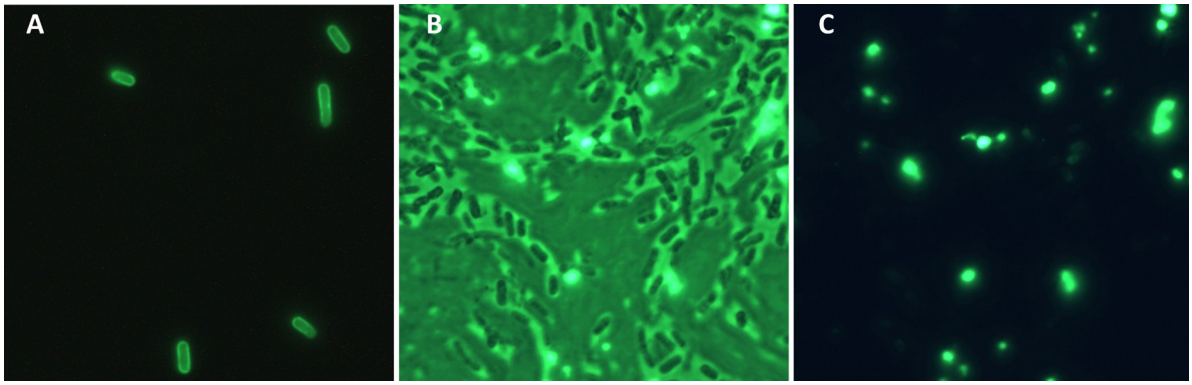


**FIG 6** (A) Fluorescence microscopy of *E. coli* MG1655 homogeneously labeled with PBD$_{KZ}$-GFP following treatment with a chloroform-saturated 0.05 M Tris-HCl (pH 7.7) buffer. (B) Phase-contrast/fluorescence overlay image of *E. coli* MG1655 in the presence of PBD$_{KZ}$-GFP and the zeamine mixture at 32 μg/ml. Gray areas represent lysed cells. (C) The corresponding fluorescence microscopy image. Zeamine treatment caused aggregates of the probe to become trapped within cellular debris.

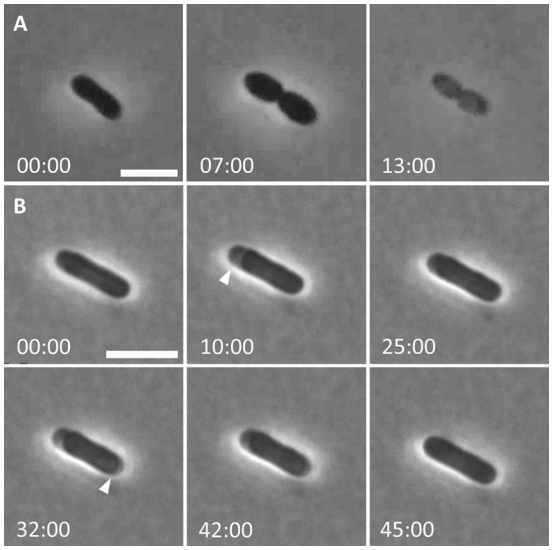


**FIG 7** Time-lapse series of the effect of the zeamines on *E. coli* MG1655. (A) Upon exposure to the zeamine antibiotics at 2× MIC (16 μg/ml), cells became slightly more spherical before losing their cell content. An intact sacculus remained, suggesting that membrane integrity rather than peptidoglycan integrity was affected. (B) In M medium, a medium with higher osmolarity, zeamine treatment (32 μg/ml) caused a transient plasmolysis-like effect, inducing shrinking of the cytoplasm (white arrowheads). The scale bar indicates 4 μm. Time points (in minutes:seconds) are indicated.

probe NPN in a dose-dependent manner. The concentrations required to induce NPN uptake were in the same range as those that evoke CF release. It is interesting that a higher concentration of zeamine II was required to induce NPN uptake than that for the zeamine mixture. This is consistent with the lower antimicrobial activity of zeamine II and suggests that the valine-linked polyketide moiety plays an important role in the destabilization of the OM. Presumably, this moiety enables stronger or other interactions with OM constituents, facilitating the integration of zeamine and zeamine I into the membrane. The fact that the bulky hydrophilic fusion protein $PBD_{KZ}$-GFP was not able to cross the OM and bind to its peptidoglycan substrate upon zeamine exposure under the tested conditions points to subtle alterations of the OM rather than drastic perturbations or discrete pore formation. At concentrations well above the MIC, the zeamines were shown to induce membrane solubilization and lysis. Detailed observation of morphological changes in zeamine-treated *E. coli* cells using time-lapse microscopy confirmed that at concentrations equivalent to 2× MIC, cell lysis occurred. Since the affected cells retain an intact peptidoglycan sacculus, this is believed to be a consequence of membrane permeabilization. In medium with higher osmolarity, cells displayed transient plasmolysis-like effects upon zeamine exposure.

Both structurally and functionally, the zeamines share similarities with cationic antimicrobial peptides (CAMPs). CAMPs are a large group of bioactive peptides produced by virtually all species of life as a major part of their primary defense system (25, 26). In addition to their broad spectrum of activity against bacteria, fungi, parasites, viruses, and even cancer cells, they display a variety of immunomodulatory effects (27). CAMPs typically are between 12 and 50 amino acids in length. They are rich in hydrophobic residues and contain an excess of basic lysine and arginine residues, which confer a net positive charge of +2 to +9 (28). Upon contact with lipid bilayers, CAMPs adopt various amphipathic structures that form the basis for their mode of action (29). They cross the OM of Gram-negative bacteria by interacting with the negatively charged phosphate groups of the LPS layer and competitively displacing the native stabilizing divalent cations. This causes local disruptions and enables translocation across the OM. The CAMPs then bind to the anionic lipid head groups of the cytoplasmic membrane and insert themselves into the outer leaflet, parallel to the plane of the bilayer, leading to the displacement of lipids. Through hydrophobic interactions, they subsequently insert themselves into the membrane interior (25). Similar to the zeamines, CAMPs exhibit a strong preference for negatively charged bacterial over zwitterionic eukaryotic membranes. Different models have been proposed to explain the process of membrane disruption, including the carpet, the toroidal pore, the barrel-stave, and the aggregate model (30–33). CAMPs effect their bactericidal action either by direct interference with the physical integrity of the membrane (membrane lysis), by inhibition of membrane-associated processes like cell division, peptidoglycan biosynthesis, or energy generation, or by translocation across the cytoplasmic membrane and interaction with (polyanionic) intracellular targets, such as DNA, RNA, or certain phosphorylated proteins (25, 28). CAMPs often combine several of the aforementioned mechanisms, targeting multiple processes with low affinity rather than interacting with one specific target with high affinity (34).

Given the presence of several primary amino and hydroxyl groups evenly distributed across the hydrophobic backbone, the zeamines might be able to adopt a membrane-bound amphipathic secondary structure in a manner similar to that of CAMPs. We speculate that the positively charged amino groups interact with the polyanionic LPS, inducing local perturbations that allow the zeamines to pass the OM. Contact with the cytoplasmic membrane likely is initiated through electrostatic interactions as well. The positively charged amino groups may be oriented toward the negatively charged phospholipid head groups, while the hydrophobic backbone is buried in the fatty acid portion. The additional positive charge present in the valine-derived moiety of zeamine and zeamine I might contribute to the stabilization of the interaction with the outer and/or cytoplasmic membrane. Upon insertion into the interior of the membrane, the zeamines could span the entire bilayer given their length. The possibility that these antimicrobial metabolites subsequently cross the cytoplasmic membrane and interact with a secondary intracellular target cannot be excluded at this stage. Future molecular dynamics simulations and membrane modeling studies may shed more light on the secondary structure adopted by the zeamines and on the precise molecular events that occur upon contact with the cell envelope. The potent, broad-spectrum activity of the zeamines against Gram-negative and Gram-positive bacteria, including multidrug-resistant pathogens, makes them attractive candidates for clinical drug development. However, their activity on eukaryotic model membranes, although reduced compared to that on bacterial artificial membranes, might limit them to topical rather than systemic applications. Further experiments are in progress to investigate rates and mechanisms of resistance development against the zeamine antibiotics.

## ACKNOWLEDGMENTS

We acknowledge Jan Balzarini for access to the cytostatic activity assay. We thank William Cenens for assistance with the time-lapse microscopy experiments.

This study was performed in the framework of the FWO "BaSeics" Research Community (W0.014.12N).

J.M. was supported by a Ph.D. scholarship from the Research Fund–Flanders (FWO).

## REFERENCES

1. **Ruiz B, Chávez A, Forero A, García-Huante Y, Romero A, Sánchez M, Rocha D, Sánchez B, Rodríguez-Sanoja R, Sánchez S, Langley E.** 2010. Production of microbial secondary metabolites: regulation by the carbon source. Crit Rev Microbiol **36:**146–167. http://dx.doi.org/10.3109/10408410903489576.
2. **Osbourn A.** 2010. Secondary metabolic gene clusters: evolutionary toolkits for chemical innovation. Trends Genet **26:**449–457. http://dx.doi.org/10.1016/j.tig.2010.07.001.
3. **Van Houdt R, Moons P, Jansen A, Vanoirbeek K, Michiels CW.** 2005. Genotypic and phenotypic characterization of a biofilm-forming Serratia plymuthica isolate from a raw vegetable processing line. FEMS Microbiol Lett **246:**265–272. http://dx.doi.org/10.1016/j.femsle.2005.04.016.
4. **Masschelein J, Mattheus W, Gao L-J, Moons P, Van Houdt R, Uytterhoeven B, Lamberigts C, Lescrinier E, Rozenski J, Herdewijn P, Aertsen A, Michiels C, Lavigne R.** 2013. A PKS/NRPS/FAS hybrid gene cluster from Serratia plymuthica RVH1 encoding the biosynthesis of three broad spectrum, zeamine-related antibiotics. PLoS One **8:**e54143. http://dx.doi.org/10.1371/journal.pone.0054143.
5. **Van Houdt R, Izquierdo JA, Aertsen A, Masschelein J, Lavigne R, Taghavi S, Michiels C, Van der Lelie D.** 2014. Genome sequence of Serratia plymuthica RVH1, isolated from a raw vegetable processing line. Genome Announc **2:**e00021–14. http://dx.doi.org/10.1128/genomeA.00021-14.
6. **Masschelein J, Clauwers C, Awodi UR, Stalmans K, Vermaelen W, Lescrinier E, Aertsen A, Michiels C, Challis GL, Lavigne R.** 15 October 2014. A combination of polyunsaturated fatty acid, nonribosomal peptide and polyketide biosynthetic machinery is used to assemble the zeamine antibiotics. Chem Sci http://dx.doi.org/10.1039/C4SC01927J.
7. **Zhou J, Zhang H, Wu J, Liu Q, Xi P, Lee J, Liao J, Jiang Z, Zhang LH.** 2011. A novel multidomain polyketide synthase is essential for zeamine production and the virulence of *Dickeya zeae*. Mol Plant Microbe Interact **24:**1156–1164. http://dx.doi.org/10.1094/MPMI-04-11-0087.
8. **Moons P.** 2008. Influence of the *Serratia plymuthica* RVH1 quorum sensing system on biofilm formation and interspecies interactions. Ph.D. thesis. KU Leuven, Heverlee, Belgium.
9. **Van Houdt R, Moons P, Aertsen A, Jansen A, Vanoirbeek K, Daykin M, Williams P, Michiels CW.** 2007. Characterization of a luxI/luxR type quorum sensing system and N-acyl homoserine lactone-dependent regulation of exo-enzyme and antibacterial component production in Serratia plymuthica RVH1. Res Microbiol **158:**150–158. http://dx.doi.org/10.1016/j.resmic.2006.11.008.
10. **Moons P, Van Houdt R, Aertsen A, Vanoirbeek K, Engelborghs Y, Michiels CW.** 2006. Role of quorum sensing and antimicrobial component production by Serratia plymuthica in formation of biofilms including mixed biofilms with Escherichia coli. Appl Environ Microbiol **72:**7294–7300. http://dx.doi.org/10.1128/AEM.01708-06.
11. **Ames BN.** 1966. Assay of inorganic phosphate, total phosphate and phosphatases. Methods Enzymol **8:**115–118. http://dx.doi.org/10.1016/0076-6879(66)08014-5.
12. **Epand RF, Epand RM, Monaco V, Stoia S, Formaggio F, Crisma M, Toniolo C.** 1999. The antimicrobial peptide trichogin and its interaction with phospholipid membranes. Eur J Biochem **266:**1021–1028. http://dx.doi.org/10.1046/j.1432-1327.1999.00945.x.
13. **Trombetta D, Castelli F, Sarpietro MG, Venuti V, Cristani M, Daniele C, Saija A, Mazzanti G, Bisignano G.** 2005. Mechanisms of antibacterial action of three monoterpenes. Antimicrob Agents Chemother **49:**2474–2478. http://dx.doi.org/10.1128/AAC.49.6.2474-2478.2005.
14. **Loh B, Grant C, Hancock REW.** 1984. Use of the fluorescent probe 1-N-phenylnaphtylamine to study the interactions of aminoglycoside antibiotics with the outer membrane of *Pseudomonas aeruginosa*. Antimicrob Agents Chemother **26:**546–551. http://dx.doi.org/10.1128/AAC.26.4.546.
15. **Briers Y, Schmelcher M, Loessner MJ, Hendrix J, Engelborghs Y, Volckaert G, Lavigne R.** 2009. The high-affinity peptidoglycan binding domain of *Pseudomonas* phage endolysin KZ144. Biochem Biophys Res Commun **383:**187–191. http://dx.doi.org/10.1016/j.bbrc.2009.03.161.
16. **Briers Y, Walmagh M, Lavigne R.** 2011. Use of bacteriophage endolysin EL188 and outer membrane permeabilizers against *Pseudomonas aeruginosa*. J Appl Microbiol **110:**778–785. http://dx.doi.org/10.1111/j.1365-2672.2010.04931.x.
17. **Briers Y, Cornelissen A, Aertsen A, Hertveldt K, Michiels CW, Volckaert G, Lavigne R.** 2008. Analysis of outer membrane permeability of *Pseudomonas aeruginosa* and bactericidal activity of endolysins KZ144 and EL188 under high hydrostatic pressure. FEMS Microbiol Lett **280:**113–119. http://dx.doi.org/10.1111/j.1574-6968.2007.01051.x.
18. **Lavigne R, Briers Y, Hertveldt K, Robben J, Volckaert G.** 2004. Identification and characterization of a highly thermostable bacteriophage lysozyme. Cell Mol Life Sci **61:**2753–2759. http://dx.doi.org/10.1007/s00018-004-4301-y.
19. **Joseleau-Petit D, Liébart JC, Ayala JA, D'Ari R.** 2007. Unstable Escherichia coli L forms revisited: growth requires peptidoglycan synthesis. J Bacteriol **189:**6512–6520. http://dx.doi.org/10.1128/JB.00273-07.
20. **Cenens W, Mebrhatu MT, Makumi A, Ceyssens PJ, Lavigne R, Van Houdt R, Taddei F, Aertsen A.** 2013. Expression of a novel P22 ORFan gene reveals the phage carrier state in *Salmonella typhimurium*. PLoS Genet **9:**e1003269. http://dx.doi.org/10.1371/journal.pgen.1003269.
21. **Huijbregts RP, de Kroon AI, de Kruijff B.** 2000. Topology and transport of membrane lipids in bacteria. Biochim Biophys Acta **1469:**43–61. http://dx.doi.org/10.1016/S0304-4157(99)00014-3.
22. **Helander IM, Mattila-Sandholm T.** 2000. Fluorometric assessment of Gram-negative bacterial permeabilization. J Appl Microbiol **88:**213–219. http://dx.doi.org/10.1046/j.1365-2672.2000.00971.x.
23. **Nikaido H.** 2003. Molecular basis of bacterial outer membrane permeability revisited. Microbiol Mol Biol Rev **67:**593–656. http://dx.doi.org/10.1128/MMBR.67.4.593-656.2003.
24. **Zasloff M.** 2002. Antimicrobial peptides of multicellular organisms. Nature **415:**389–395. http://dx.doi.org/10.1038/415389a.
25. **Afacan NJ, Yeung AT, Pena OM, Hancock REW.** 2012. Therapeutic potential of host defense peptides in antibiotic-resistant infections. Curr Pharm Des **18:**807–819. http://dx.doi.org/10.2174/138161212799277617.
26. **Nguyen LT, Haney EF, Vogel HJ.** 2011. The expanding scope of antimicrobial peptide structures and their modes of action. Trends Biotechnol **29:**464–472. http://dx.doi.org/10.1016/j.tibtech.2011.05.001.
27. **Haney EF, Hancock REW.** 2013. Peptide design for antimicrobial and immunomodulatory applications. Biopolymers **100:**572–583. http://dx.doi.org/10.1002/bip.22250.
28. **Fjell CD, Hiss JA, Hancock RE, Schneider G.** 2012. Designing antimicrobial peptides: form follows function. Nat Rev Drug Discov **11:**37–51. http://dx.doi.org/10.1038/nrd3591.
29. **Hancock REW.** 2001. Cationic peptides: effectors in innate immunity and novel antimicrobials. Lancet Infect Dis **1:**156–164. http://dx.doi.org/10.1016/S1473-3099(01)00092-5.
30. **Pouny Y, Rapaport D, Mor A, Nicolas P, Shai Y.** 1992. Interaction of antimicrobial dermaseptin and its fluorescently labelled analogs with phospholipid membranes. Biochemistry **31:**12416–12423. http://dx.doi.org/10.1021/bi00164a017.
31. **Matsuzaki K, Murase O, Fujii N, Miyajima K.** 1996. An antimicrobial peptide, magainin 2, induced rapid flip-flop of phospholipids coupled with pore formation and peptide translocation. Biochemistry **35:**11361–11368. http://dx.doi.org/10.1021/bi960016v.
32. **Ehrenstein G, Lecar H.** 1977. Electrically gated ionic channels in lipid bilayers. Q Rev Biophys **10:**1–34. http://dx.doi.org/10.1017/S0033583500000123.
33. **Wu MH, Maier E, Benz R, Hancock REW.** 1999. Mechanism of interaction of different classes of cationic antimicrobial peptides with planar bilayers and with the cytoplasmic membrane of *Escherichia coli*. Biochemistry **38:**7235–7242. http://dx.doi.org/10.1021/bi9826299.
34. **Nijnik A, Hancock REW.** 2009. Host defence peptides: antimicrobial and immunomodulatory activity and potential applications for tackling antibiotic-resistant infections. Emerg Health Threats J **2:**e1. http://dx.doi.org/10.3134/ehtj.09.001.